

Deep Reinforcement Learning of Marked Temporal Point Processes

Utkarsh Upadhyay, Abir De, and Manuel Gomez-Rodriguez

Max Planck Institute for Software Systems
`{utkarshu, ade, manuelgr}@mpi-sws.org`

Abstract

In a wide variety of applications, humans interact with a complex environment by means of asynchronous stochastic discrete events in continuous time. Can we design online interventions that will help humans achieve certain goals in such asynchronous setting? In this paper, we address the above problem from the perspective of deep reinforcement learning of marked temporal point processes, where both the actions taken by an *agent* and the feedback it receives from the *environment* are asynchronous stochastic discrete events characterized using marked temporal point processes. In doing so, we define the agent’s policy using the intensity and mark distribution of the corresponding process and then derive a flexible policy gradient method, which embeds the agent’s actions and the feedback it receives into real-valued vectors using deep recurrent neural networks. Our method does not make any assumptions on the functional form of the intensity and mark distribution of the feedback and it allows for arbitrarily complex reward functions. We apply our methodology to two different applications in personalized teaching and viral marketing and, using data gathered from Duolingo and Twitter, we show that it may be able to find interventions to help learners and marketers achieve their goals more effectively than alternatives.

1 Introduction

In recent years, the framework of marked temporal point processes (MTPPs) [1] has become increasingly popular for modeling asynchronous event data in continuous time, which is ubiquitous in a wide range of application domains, from social and information networks to finance or health informatics. For example, in social and information networks, events may represent users’ posts, clicks or likes; in finance, they may represent buying and selling orders; or, in health informatics, they may represent when a patient exhibits different symptoms or receives treatment. In most cases, the development of a new model reduces to the problem of designing an appropriate functional form for the conditional intensity (or intensities) of the events of interest as well as the distribution of the corresponding mark(s).

In this context, a recent line of work [13, 27, 29, 30, 33, 34] has exploited an alternative view of MTPPs as stochastic differential equations (SDEs) with jumps [10] to design online, adaptive interventions using stochastic optimal control. While this line of work has shown promise at enhancing the functioning of social and information systems, their wide spread use and deployment is precluded mainly by two drawbacks. First, they make strong assumptions about the functional form of the conditional intensities and mark distributions of the MTPPs, which in turn prevent them from using state of the art MTPP models based on deep learning [5, 11, 17]. Second, the objective functions that the interventions optimize upon, need to be carefully chosen to ensure that the underlying stochastic optimal control problem remains tractable. As a consequence,

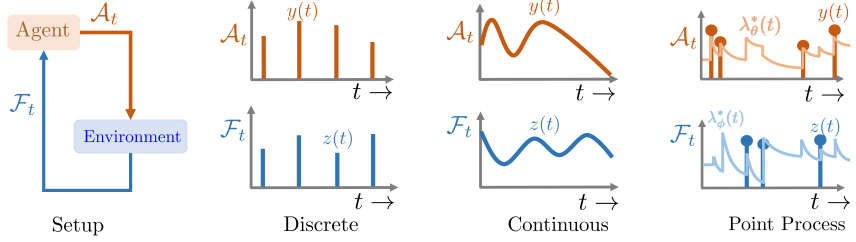


Figure 1: Reinforcement learning setups. In the traditional discrete time setting [26], actions and feedback occur in discrete time; in the continuous time setting [4], actions and feedback are real value functions in continuous time; and, in the marked temporal point process setting (our work), actions and feedback are asynchronous events localized in continuous time.

the use of (more) meaningful objective functions with clear semantics is often off limits. In our work, we overcome these drawbacks by approaching the problem from the perspective of deep reinforcement learning of MTPPs.

More specifically, we first introduce a novel reinforcement learning problem where both the actions taken by an *agent* and the feedback it receives from its *environment* are asynchronous stochastic events in continuous time, which are characterized using MTPPs. Here, the goal is finding the *optimal* intensity and mark distribution for the agent’s actions—the optimal policy—that maximize an arbitrary reward function, which may depend on its actions and the feedback. Then, we derive a novel policy gradient method, specially designed to solve the above problem, which embeds the agent’s actions and the feedback from the environment into real-valued vectors using deep recurrent neural networks (RNNs). In contrast with the literature on stochastic optimal control of SDEs with jumps, our method does not make any assumptions on the functional form of the conditional intensity (or intensities) and mark distribution(s) characterizing the feedback, and it allows for arbitrarily complex reward functions. Moreover, it departs from previous work in the reinforcement learning literature [4, 6, 8, 9, 15, 20, 26, 28, 31] in two key aspects, which are also illustrated in Figure 1:

- I. The agent’s actions and environment’s feedback are asynchronous stochastic events in continuous time. In contrast, previous work has considered synchronous actions and (potentially delayed) feedback in discrete time [6, 15, 20, 31], with few notable exceptions [4, 9, 28]. While these exceptions considered continuous time, they assumed actions and feedback to be continuous and deterministic and the dynamics of the environment to be known.¹
- II. Our policy is a conditional intensity function (and a mark distribution), which is used to *sample* the times (and marks) of the agent’s actions. Here, note that a sampled agent’s action may need to be resampled due to the occurrence of new feedback events before the sampled time. In contrast, previous works considered the policy to be a probability distribution or, more rarely, a deterministic function [4, 9, 28].

Finally, we apply our methodology to two different applications in personalized teaching [14, 22, 27] and viral marketing [12, 25, 29, 33, 34], respectively. For *simple* dynamics and objective functions, which allow for stochastic optimal control approaches, our method achieves a comparable performance even though it does not have access to the true underlying dynamics. For *complex* dynamics and/or objective functions, which do not allow for stochastic optimal control approaches, our method is able to successfully find interventions that optimize the corresponding objective function and beat several competitive baselines. To facilitate research in temporal point processes within the reinforcement learning community at large, we are releasing an open-source

¹Our setting should not be confused with the *asynchronous* setting of Mnih *et al.* [20], where the gradient descent is asynchronous but the action/observations are synchronous and the system evolves at discrete time steps.

implementation of our method in TensorFlow as well as synthetic and real-world data used in our experiments.²

2 Problem formulation

In this section, we first briefly revisit the theoretical framework of marked temporal point processes [1] and then use it to formally define our novel reinforcement learning problem, where an agent interacts with a complex environment by means of asynchronous stochastic discrete events in continuous time.

Marked temporal point processes. A marked temporal point process (MTPP) is a random process whose realization consists of an ordered sequence of events localized in time, *i.e.*,

$$\mathcal{H} = \{e_0 = (t_0, z_0), e_1 = (t_1, z_1), \dots, e_n = (t_n, z_n)\},$$

where $t_i \in \mathbb{R}^+$ is the time of occurrence of event $i \in \mathbb{Z}$ and $z_i \in \mathcal{Z}$ is the associated mark. The actual meaning of the events varies across applications, *e.g.* in social networks, t_i may represent the time when a message is posted, clicked or liked, z_i may represent the type of interaction, the message content, or its polarity, and the domain of the marks \mathcal{Z} is application dependent. Here, we characterize the event times of a MTPP using a conditional intensity function $\lambda^*(t)$, which is the probability of observing an event in the time window $[t, t + dt)$ given the events history $\mathcal{H}_t = \{e_i = (t_i, z_i) \in \mathcal{H} \mid t_i < t\}$, *i.e.*,

$$\lambda^*(t) := \mathbb{P}\{\text{event in } [t, t + dt) \mid \mathcal{H}_t\}, \quad (1)$$

where the sign * means that the intensity may depend on the history \mathcal{H}_t . Moreover, we characterize the marks of the events using a distribution $m(z \mid \mathcal{H}_t) = m^*(z)$, which is the probability that mark z is selected, *if* an event has occurred at time t . Then, we can compute the likelihood of a history of events $\mathcal{A}_T \subseteq \mathcal{H}_T$ as:

$$\mathbb{P}(\mathcal{A}_T) := \left(\prod_{e_i \in \mathcal{A}_T} \underbrace{\lambda^*(t_i)}_{\substack{\text{Prob. of an action at } t_i}} \underbrace{m^*(z_i)}_{\substack{\text{Prob. of mark } z_i}} \right) \overbrace{\exp \left(- \int_0^T \lambda^*(s) ds \right)}^{\substack{\text{Prob. of no actions at } t \in [0, T] \setminus \{t_i\}}} . \quad (2)$$

In the remainder of the paper, whenever an intensity function and mark distribution are parametrized by θ , we write $\lambda_\theta^*(\cdot)$, $m_\theta^*(\cdot)$, $\mathbb{P}_\theta(\mathcal{A}_T)$, and, for notational simplicity, use $p_\theta^* = (\lambda_\theta^*, m_\theta^*)$ as a short-hand to denote the joint probability density of the MTPP. Recent literature [5, 8, 12, 13, 17, 30, 33] has established that MTPPs outperform other models (*e.g.*, exponential law) in their ability to accurately predict online and off-line human actions.

Reinforcement learning of marked temporal point processes. Assume there is an agent who takes actions in a complex environment and the environment also provides feedback to the agent over time. Moreover, both the actions and the feedback are asynchronous stochastic events localized in time and thus we characterize them using marked temporal point processes (MTPPs), *i.e.*,

- *Action events:* $\mathcal{A} = \{e_i = (t_i, y_i)\}$, where $(t_i, y_i) \sim p_{\mathcal{A}; \theta}^* = (\lambda_\theta^*, m_\theta^*)$
- *Feedback events:* $\mathcal{F} = \{f_i = (t_i, z_i)\}$, where $(t_i, z_i) \sim p_{\mathcal{F}; \phi}^* = (\lambda_\phi^*, m_\phi^*)$

In the above characterization, we allow the joint probability densities $p_{\mathcal{A}; \theta}^*$ and $p_{\mathcal{F}; \phi}^*$ to depend on the joint history of events $\mathcal{H}_t := \mathcal{A}_t \cup \mathcal{F}_t$. Finally, after a *cut-off* time T , we assume that the

²<https://github.com/Networks-Learning/tpprl>

agent receives an arbitrary (stochastic) reward $R^*(T)$, which may depend on the agent’s actions \mathcal{A}_T and the environment’s feedback \mathcal{F}_T .

Given the above problem setting, we can formally define our reinforcement learning (RL) problem for marked temporal point processes as follows:

Problem definition. *Given an agent with $p_{\mathcal{A};\theta}^* = (\lambda_\theta^*, m_\theta^*)$, an environment with $p_{\mathcal{F};\phi}^* = (\lambda_\phi^*, m_\phi^*)$ and an arbitrary stochastic reward $R^*(T)$, the goal is to find the optimal action intensity and mark distribution—the optimal policy—that maximize the expected reward. Formally,*

$$\underset{p_{\mathcal{A};\theta}^*(\cdot)}{\text{maximize}} \quad \mathbb{E}_{\mathcal{A}_T \sim p_{\mathcal{A};\theta}^*(\cdot), \mathcal{F}_T \sim p_{\mathcal{F};\phi}^*(\cdot)} [R^*(T)], \quad (3)$$

where the expectation is taken over all possible realizations of the marked temporal point processes associated to the agent’s action events and the environment’s feedback events. In the remainder of the paper, we will denote the optimal policy using $\pi^*(\theta) = \text{argmax}_{p_{\mathcal{A};\theta}^*(\cdot)} \mathbb{E}[R^*(T)]$.

Note that the above definition departs from previous work on reinforcement learning [4, 6, 9, 15, 20, 26, 28, 31] in several ways. First, the agent’s actions and environment’s feedback are asynchronous stochastic events in continuous time. Moreover, note that the agent may receive feedback from the environment asynchronously at any time, not only after each of its actions. This is in contrast with previous work in the literature, which has only considered synchronous actions (and potentially delayed) feedback in discrete time (or, in some cases, continuous actions and feedback), as illustrated in Figure 1. Second, our policy is defined by a conditional intensity function (and a mark distribution), which is used to *sample* the times (and marks) of the agent’s actions. Here, note that a sampled agent’s action may need to be resampled due to the occurrence of new feedback events before the sampled time. In contrast, previous work has used probability distributions (or, in some cases, deterministic functions) as policies.

Remarkably, the above problem definition naturally fits numerous problems in a wide variety of application domains, particularly in the context of social and information online systems. For example, in personalized teaching in online learning platforms, the platform that shows content items to learners is the agent, the platform takes an action when it shows an item to a learner, the learners are the environment, and the probability that the learner recalls an item defines the reward. In viral marketing in social networks, a user who aims to increase the visibility of her posts is the agent, the user takes an action when she posts a message, her followers’ feeds form the environment and the visibility (or attention) she receives defines the reward. In all these cases, the environment distribution $p_{\mathcal{F};\phi}^*$ may be highly complex and thus our policy gradient method will only assume that it can sample from $p_{\mathcal{F};\phi}^*$. In other words, the environment distribution will be considered a *black box*.

3 Proposed policy gradient method

In this section, we tackle the reinforcement learning problem defined by Eq. 3 using a novel policy gradient method for marked temporal point processes. More specifically, we first leverage recurrent neural networks (RNNs) to parametrize the policy $p_{\mathcal{A};\theta}^*$ and then use stochastic gradient descent (SGD) to find the policy parameters θ that maximizes the expected reward $\mathbb{E}[R^*]$.

Policy parametrization. In many application domains, at any time t , the (optimal) policy $p_{\mathcal{A};\theta}^*$ that maximizes the reward may depend on the previous history of the action events and the feedback events, $\mathcal{H}_t = \mathcal{A}_t \cup \mathcal{F}_t$, in an unknown and complex way. To capture such dependence, we parametrize the policy $p_{\mathcal{A};\theta}^*$ using a recurrent neural network (RNN), where we embed both the actions events and the feedback events into real-valued vectors \mathbf{h} , similarly as in several

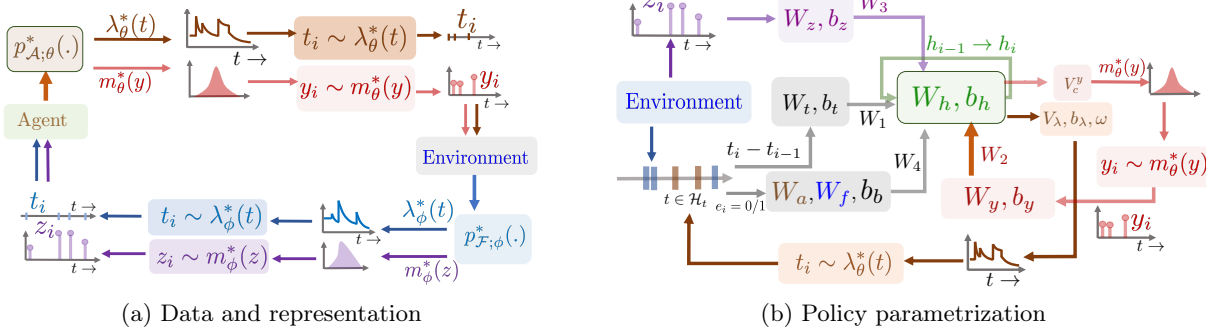


Figure 2: Reinforcement learning (RL) of marked temporal point processes (MTPPs). Panel (a) shows the type of data and representation used in RL of MTPPs. Panel (b) shows the policy parametrization used by our policy gradient method.

recent state of the art MTPP deep learning models [5, 11, 17]³. Next, we elaborate further on our architecture⁴, which we also summarize in Figure 2, and then discuss how to efficiently sample action events from the (optimal) policy.

— *Input layer*. After the i -th event occurs, be it an action event or a feedback event, the input layer converts the associated information, *i.e.*, the time t_i , the marker z_i (or y_i), and the type of event $e_i \in \{0, 1\}$, where $e_i = 0$ denotes action and $e_i = 1$ denotes feedback, into compact vectors. Specifically, it computes:

$$\begin{aligned}\boldsymbol{\tau}_i &= \mathbf{W}_t(t_i - t_{i-1}) + \mathbf{b}_t, & \mathbf{y}_i &= \mathbf{W}_y y_i + \mathbf{b}_y \text{ if } e_i = 0 \\ \mathbf{b}_i &= \mathbf{W}_a(1 - e_i) + \mathbf{W}_f e_i + \mathbf{b}_b, & \mathbf{z}_i &= \mathbf{W}_z z_i + \mathbf{b}_z \text{ if } e_i = 1\end{aligned}$$

where \mathbf{W}_\bullet , \mathbf{b}_t , \mathbf{b}_y , \mathbf{b}_z and \mathbf{b}_b are trainable weights. Moreover, note that we encode the action marks y_i and feedback marks z_i separately since they may belong to different domains. To this aim, one of the inputs y_i and z_i will be marked as *absent* using sentinel values depending on whether $e_i = 0$ or $e_i = 1$, respectively. Finally, these signals are fed into the hidden layer, which we describe next.

— *Hidden layer*. This layer iteratively updates the latent embedding \mathbf{h}_{i-1} , by taking inputs of previous events from the input layer:

$$\mathbf{h}_i = \tanh(\mathbf{W}_h \mathbf{h}_{i-1} + \mathbf{W}_1 \boldsymbol{\tau}_i + \mathbf{W}_2 \mathbf{y}_i + \mathbf{W}_3 \mathbf{z}_i + \mathbf{W}_4 \mathbf{b}_i + \mathbf{b}_h), \quad (4)$$

where \mathbf{W}_\bullet and \mathbf{b}_h are trainable weights.

— *Output layer*. The output layer computes the policy $p_{A;\theta}^* = (\lambda_\theta^*, m_\theta^*)$, *i.e.*, the intensity function λ_θ^* and the mark distribution m_θ^* . Assume the agent has generated i events by time t , then, the output layer computes the intensity as:

$$\lambda_\theta^*(t) = \exp(b_\lambda + w_t(t - t_i) + \mathbf{V}_\lambda \mathbf{h}_i) \quad (5)$$

where \mathbf{V}_λ , b_λ and w_t are trainable weights and t_i denotes the time of the i -th action event. Here, the b_λ encodes a base intensity level for the occurrence of the $(i+1)$ -th action event, the term $w_t(t - t_i)$ encodes the influence of the i -th action event, and the term \mathbf{V}_λ encodes the influence

³Note that previous MTPP deep learning models aims to provide event predictions. This is contrast with the current work, which aims to provide optimal event interventions.

⁴Depending on the application domains, action events or feedback events may not contain marks and, thus, the architecture may be slightly simpler.

Algorithm 1: Returns the next action time

```

1: Input: Parameters  $b_\lambda, w_t, \mathbf{V}_\lambda, \mathbf{h}_i$ , last event time  $t'$ 
2: Output: Next action time  $t$ 
3:  $CDF(\bullet) \leftarrow$  Cumulative distribution of next arrival time
4:  $u \leftarrow \text{UNIF}[0, 1]$ 
5:  $t \leftarrow CDF^{-1}(u)$ 
6: while  $t < T$  do
7:    $(s, z) \leftarrow \text{WAITUNTILNEXTFEEDBACK}(t)$ 
8:   if feedback arrived before  $t$  then
9:      $CDF(\bullet) \leftarrow \text{MODIFY}(CDF(\bullet), s, z)$ 
10:     $t \leftarrow CDF^{-1}(u)$ 
11:   else
12:     return  $t$ 
13:   end if
14: end while
15: return  $t$ 

```

of previous events. The particular choice of mark distribution m_θ^* depends on the application domain. Here, we experiment with discrete marks and thus model the marks using a multinomial distribution, *i.e.*,

$$\mathbb{P}[y_{i+1} = c] = \frac{\exp(\mathbf{V}_{c,:}^y \mathbf{h}_i)}{\sum_{l \in \mathcal{Y}} \exp(\mathbf{V}_{l,:}^y \mathbf{h}_i)}, \quad (6)$$

where \mathcal{Y} denote the domain of the marks and \mathbf{V}^y are trainable weights.

Sampling action events from the policy. To implement the above policy $p_{\mathcal{A};\theta}^* = (\lambda_\theta^*, m_\theta^*)$, we need to be able to sample the action times t and marks y from the intensity function defined by Eq. 5 and the mark distribution defined by Eq. 6, respectively. While the latter reduces to sampling from a multinomial distribution, which is straightforward, the former requires developing a novel sampling algorithm leveraging inverse transform sampling, which we describe in Algorithm 1. The details of calculating $CDF(\bullet)$ and the related modifications are provided in Appendix C.

Maximizing the expected reward. In the following, we denote the expected reward as a function of the policy parameters θ as:

$$J(\theta) = \mathbb{E}_{\mathcal{A}_T \sim p_{\mathcal{A};\theta}^*(\cdot), \mathcal{F}_T \sim p_{\mathcal{F};\phi}^*(\cdot)} [R^*(T)] \quad (7)$$

Then, we find the optimal policy $p_{\mathcal{A};\theta}^*$ that maximizes the expected reward function $J(\theta)$ using stochastic gradient descent (SGD) [23], *i.e.*, $\theta_{l+1} = \theta_l + \alpha_l \nabla_\theta J(\theta)|_{\theta=\theta_l}$. To do so, we need to compute the gradient of the expected reward function $\nabla_\theta J(\theta)$, however, this may seem challenging at first especially since the expectation is taken over realizations of marked temporal point processes. Perhaps surprisingly, we can compute such gradient using the following proposition (proved in Appendix A).

Proposition 1. *Given an agent with $p_{\mathcal{A};\theta}^* = (\lambda_\theta^*, m_\theta^*)$, an environment with $p_{\mathcal{F};\phi}^* = (\lambda_\phi^*, m_\phi^*)$, the gradient of the expected reward function $J(\theta)$ with respect to θ is given by:*

$$\nabla_\theta J(\theta) = \mathbb{E}_{\mathcal{A}_T \sim p_{\mathcal{A};\theta}^*(\cdot), \mathcal{F}_T \sim p_{\mathcal{F};\phi}^*(\cdot)} [R^*(T) \nabla_\theta \log \mathbb{P}_\theta(\mathcal{A}_T)], \quad (8)$$

where $\log \mathbb{P}_\theta(\mathcal{A}_T) = \sum_{e_i \in \mathcal{A}_T} (\log \lambda_\theta^*(t_i) + \log m_\theta^*(z_i)) - \int_0^T \lambda_\theta^*(s) ds$.

In the above proposition, the gradient of the log-likelihood of the times and marks of a realization of the marked temporal point process associated to the agent’s actions, $\nabla_\theta \log \mathbb{P}_{\mathcal{A};\theta}^*(\mathcal{H}_T)$, can be easily computed using the policy parametrization defined by Eqs. 5 and 6. Moreover, note that the proposition formally shows that the REINFORCE trick [32] is still valid if the expectation is taken over realizations of marked temporal point processes, which are a type of *random elements* [3] whose values are discrete events localized in continuous time.

Unfortunately, the above procedure does not limit the intensity of actions by the agent and this may be problematic in practice (*e.g.*, in viral marketing in social networks, a user who aims to increase the visibility of her posts may only be able to post a certain number of times). To overcome this, we consider instead a penalized expected reward function $J_r(\theta)$ with differentiable regularizers $g_\lambda(\lambda_\theta^*(t))$ and $g_m(m_\theta^*(t))$, which implicitly impose a budget on the number of action events and marks, respectively, *i.e.*,

$$J_r(\theta) = \mathbb{E}_{\mathcal{A}_T \sim p_{\mathcal{A};\theta}^*(\cdot), \mathcal{F}_T \sim p_{\mathcal{F};\phi}^*(\cdot)} \left[R^*(T) - q_l \int_0^T g_\lambda(\lambda_\theta^*(t)) - q_m \int_0^T g_m(m_\theta^*(t)) dt \right]. \quad (9)$$

The gradient of the penalized reward can be readily computed using the following proposition (proved in Appendix B):

Proposition 2. *Given an agent with $p_{\mathcal{A};\theta}^* = (\lambda_\theta^*, m_\theta^*)$, an environment with $p_{\mathcal{F};\phi}^* = (\lambda_\phi^*, m_\phi^*)$, the gradient of $J_r(\theta)$ is given by,*

$$\begin{aligned} \nabla_\theta J_r(\theta) &= \mathbb{E}_{\mathcal{A}_T \sim p_{\mathcal{A};\theta}^*(\cdot), \mathcal{F}_T \sim p_{\mathcal{F};\phi}^*(\cdot)} \left[\right. \\ &\quad \left(R^*(T) - q_l \int_0^T g_\lambda(\lambda_\theta^*(t)) - q_m \int_0^T g_m(m_\theta^*(t)) dt \right) \nabla_\theta \log \mathbb{P}_\theta(\mathcal{A}_T) \\ &\quad \left. - \left(q_l \int_0^T g'_\lambda(\lambda_\theta^*(t)) \nabla_\theta \lambda_\theta^*(t) dt + q_m \int_0^T g'_m(m_\theta^*(t)) \nabla_\theta m_\theta^*(t) dt \right) \right], \end{aligned} \quad (10)$$

where $g'_\lambda(\lambda_\theta^*(t)) = \frac{d g_\lambda(\lambda_\theta^*(t))}{d \lambda_\theta^*(t)}$ and $g'_m(m_\theta^*(t)) = \frac{d g_m(m_\theta^*(t))}{d m_\theta^*(t)}$.

In our experiments, we will approximate the expectation in Eq. (10) by first running a *batch* of realizations (or *episodes*) of the corresponding marked temporal point processes⁵ and then calculating the mean of the resulting gradients for each batch.

4 Experiments on spaced repetition

Problem definition. It is well known in the psychology literature that repeated and temporally distributed reviewing of information aids long term memorization [14, 16, 19, 18]. Following recent work in the machine learning literature [18, 22, 27], we will consider the following setting: an online learning platform needs to teach one student some number of items with varying difficulty, say, words from the vocabulary of a foreign language. To this aim, the platform interacts with the student during a studying period by asking her to *review* each item multiple times, *i.e.*, show a word to the student, ask for its translation, and then show the correct answer. Then, the goal is to help the platform decide when to ask the student to review each item to better prepare her for a *test*, which will take place sometime after the learning period is over. Under our problem definition, the online platform is the agent, it generates action events \mathcal{A} when

⁵In some applications, we may be able to play back historical data from the environment against our policy and, in other domains, we may need to resort to a (complex) environment simulator.

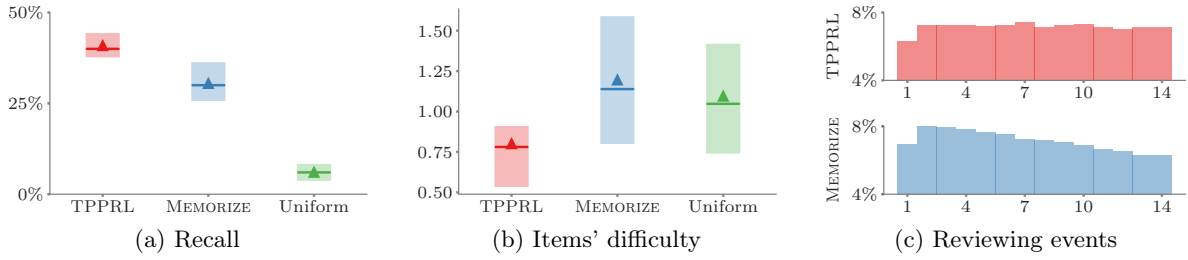


Figure 3: Spaced Repetition. Performance of our policy gradient method against MEMORIZE [27] and a uniform baseline, which follows a constant reviewing rate and chooses items uniformly at random. Panel (a) shows the empirical recall probability at time $T + \tau$ and Panel (b) shows the difficulty level of the items selected for review by different methods. In both cases, the solid horizontal line (triangle) shows the median (average) value across review sequences and the box limits correspond to the 25%-75% percentiles. All methods schedule (within a small tolerance) the same number of review events. Panel (c) compares the average fraction of review events per day across all items for our method (above) and MEMORIZE (below).

it asks a student to review an item, the student is the environment and she generates feedback events \mathcal{F} when she reviews an item, indicating whether she was able to recall the item or not, and the recall probability at the test time defines the reward.

Interestingly, the above setting has been recently studied from the point of view of stochastic optimal control [27], where the authors have derived the optimal scheduling algorithm for a set of items. However, their solution assumes that the difficulty of the items and the student model are known [24] and that the objective function—the reward—has a particular functional form which depends on the average recall probability over time (and not the actual sampled recall at test time). Here, we use our reinforcement learning method to derive (optimal) policies for arbitrarily complex and unknown student models, items with unknown difficulties and more intuitive reward definitions.

Experimental setup. Since we cannot make real interventions in an online learning platform, we use data from Duolingo to fit a probabilistic student model, as reported in previous work [24, 27], which we then use to simulate a student’s performance over time (refer to Appendix E for further details on the student model). Here, the optimal policy $p_{\mathcal{A};\theta}^* = (\lambda_\theta^*(t), m_\theta^*(t))$ comprises of a reviewing intensity function and a multinomial mark distribution. The former characterizes when to review and the latter characterizes which item to review each time. Then, we train and test our policy gradient method as follows.

Given a student model and a set of items, we train the platform’s policy $p_{\mathcal{A};\theta}^*$ by using SGD with a quadratic (entropy) regularizer on the reviewing intensity (mark distribution), *i.e.*, $g(\lambda_\theta^*(t), m_\theta^*(t)) = (\lambda_\theta^*(t))^2 + H(m_\theta^*(t))$ where $H(m_\theta^*(t_i)) := -\sum_{c \in \mathcal{Y}} \mathbb{P}[y_i = c] \log \mathbb{P}[y_i = c]$, on a training consisting of simulated reviewing and test sequences. More specifically, on iteration i , we build a batch of b reviewing (or studying) sequences of time length T , where we sample student’s recalls from the student model every time our policy $p_{\theta_i}^*$ generates a reviewing events and compute the reward at the end of each sequence. Here, the reward is the sampled recall at test time $T + \tau$, which is a natural performance measure for the goal stated in the problem definition. To test the trained model, we just generate additional reviewing sequences using the student model and the trained policy and compute the reward at the end of each sequence. Appendix D for further details on the training and testing procedure. Here, we compare the performance of our method with two alternatives: (i) a state of the art method called MEMORIZE [27] which, in

contrast with our work, has full access to the student model and is specially designed to maximize the average recall probability over time, and (ii) a baseline reviewing schedule which follows a constant reviewing rate and choose items uniformly at random.

Results. Figures 3(a-b) summarize the results, where the number of reviewing events by each method is the same. The results show that: (i) by maximizing the actual reward one is aiming for, our method is able to outperform both MEMORIZE and the baseline by large margins; and, (ii) given the limited study time, our method tends to focus on less difficult items. Finally, in Figure 3(c), we compare how our method and MEMORIZE distribute reviewing events during the studying period. While our method keeps a constant load over time, MEMORIZE provides initially a heavier studying load.

5 Experiments on smart broadcasting

Problem definition. In the smart broadcasting problem, first introduced by Spasojevic et al. [25], the goal is to help a social media user decide when to post to achieve high visibility in her followers’ feeds, *i.e.*, to elicit attention from her followers. Under our problem definition, the user is the agent, she generates action events \mathcal{A} when she posts, her followers’ feeds forms the environment, the environment generates feedback events \mathcal{F} when any of the other users her followers follow post, and the visibility she receives defines the reward. Then, the problem reduces to finding the (optimal) policy $p_{\mathcal{A};\theta}^*$ that maximizes the reward.

Following previous work [29, 33, 34], we measure visibility a user achieves, *i.e.*, the reward, using two different metrics: (i) the position of her most recent post on her followers’ feeds over time, or *rank*, *i.e.*, $R^*(T) = \int_0^T r(t)dt$, where the position zero, $r(t) = 0$, corresponds to top and thus lower is better; (ii) the (amount of) time that her most recent post is at the top of her followers’ feeds, or *time at the top*, *i.e.*, $R^*(T) = \int_0^T \mathbb{I}(r(t) < 1)dt$, and thus higher is better. If the followers’ feeds are sorted in reverse chronological order, previous work has derived optimal offline [12] and online [34] algorithms for (i) and (ii), respectively, under the additional assumption that the posting intensity of other users her followers follow adopts certain functional form. However, as pointed out by previous work, feeds are typically algorithmically sorted, the posting intensity of other users may be highly complex, and thus the derived algorithms may be of limited use in practice. Here, we use our reinforcement learning method to derive (optimal) policies for algorithmically sorted feeds and, by doing so, we are able to help users achieve higher visibility than the above algorithms. Appendix G contains additional experiments for feeds sorted in reverse chronological order.

Experimental setup. We use data gathered from Twitter as reported in previous work [2], which comprises profiles of 52 million users, 1.9 billion directed follow links among these users, and 1.7 billion public tweets posted by the collected users. The follow link information is based on a snapshot taken at the time of data collection, in September 2009. Here, we focus on the tweets published during a two month period, from July 1, 2009 to September 1, 2009, and sample 100 users uniformly at random. For each of these users, we retrieve five of her followers (chosen at random), select five other *followees* of each follower (chosen at random), and collect all the (re)tweets they published. Each follower represents a wall and our broadcaster is *competing* with the other followees of follower for attention.

Since we do not have access to the feed sorting algorithm used by Twitter, we experiment with a relatively simple sorting algorithm based on a priority queue⁶ (refer to Appendix F). Here, since our feed sorting algorithm does only depends on the time of the post and the identity of

⁶We expect that, the more complex the sorting algorithm, the larger the competitive advantage our algorithm will offer in comparison with competing methods designed for feeds sorted in reverse chronological order.

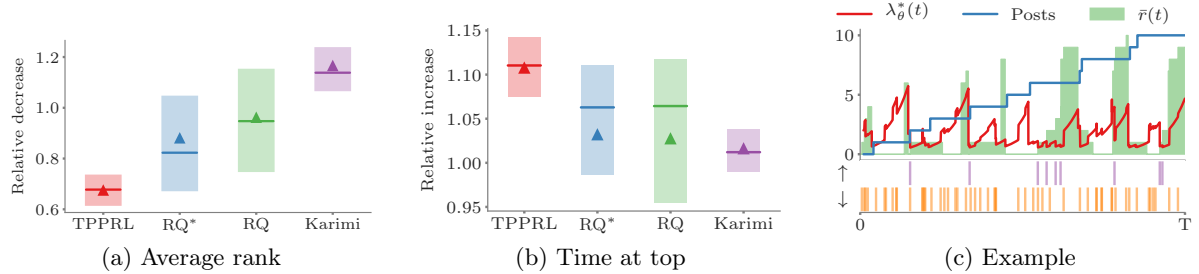


Figure 4: Smart broadcasting. Performance of our policy gradient method against REDQUEEN [34] (RQ), a variant of REDQUEEN which has access to true ranks (RQ*), and Karimi’s method [12] on feeds using a sorting algorithm based on a priority queue (refer to Appendix F). Panels (a) and (b) show the average rank and time at the top, where the solid horizontal line shows the median value across users, normalized with respect to the value achieved by a user who follows a uniform Poisson intensity, and the box limits correspond to the 25%-75% percentiles. For the average rank, lower is better and, for time at the top, higher is better. In both cases, the number of messages posted by each method is the same. Panel (c) shows a user’s intensity $\lambda_\theta^*(\cdot)$ (in blue), as provided by our method, the counts of the user’s posts (in green), the average rank (in red), the posting times of a competing user with higher priority (in purple), and the posting times of another competing user with lower priority (in yellow).

the user who posts, not marks (*e.g.*, content of the post), the optimal policy only comprises an intensity function, *i.e.*, $p_{\mathcal{A};\theta}^* = \lambda_\theta^*(t)$. Then, we train and test our policy gradient method as follows.

For each user, we divide her feedback events, *i.e.*, the posts by other users her followers follow, into a training set and a test set. The latter contains all feedback events generated in a time window of length T at the end of the recording period and the former contains all other feedback events. Here, we set the length T such that the overall expected number of events in the test set is ~ 200 . Then, we train each user’s policy $\lambda_\theta^*(t)$ by using stochastic gradient descent (SGD) with a quadratic regularizer $g(\lambda^*(t)) = (\lambda^*(t))^2$. More specifically, on each iteration i , we build a batch of b sequences of length T , taken uniformly at random from the training set, we *replay* the feedback events from these sequences while interleaving the posts generated by our policy $\lambda_{\theta_i}^*$, and compute the reward at the end of each sequence. To test the trained policy $\lambda_\theta^*(t)$, we just replay the feedback events from the test set while interleaving the posts generated by the policy and compute the reward at the end of the sequence. Appendix D contain additional implementation details.

In the above, we experiment both with rank and time at the top as rewards and compare our method with two state of the art methods, REDQUEEN [34] and the method by Karimi et al. [12]. The former is an online algorithm specially designed to minimize the average rank in feeds sorted in reverse chronological order and the latter is an offline algorithm specially designed to maximize the time at the top in feeds sorted in reverse chronological order. However, because REDQUEEN assumes that the feed is inverse chronologically sorted and posts with intensity $\propto \text{rank}_{\text{chrono}}(t)$, we also compare our method TPPRL against a stronger heuristic RQ*, which posts with intensity $\propto \text{rank}_{\text{priority}}(t)$.

Results. Figures 4(a-b) summarize the results, where the number of messages posted by each method is the same and all rewards are normalized by the reward achieved by a baseline user who follows a uniform Poisson intensity. The results show that, by not making any assumption about the feed sorting algorithm, our method is able to outperform both REDQUEEN and Karimi’s

method, which were specially designed to minimize the average rank and time at the top in feeds sorted in reverse chronological order, respectively. Moreover, our method provides solutions with smaller variance in performance than REDQUEEN. Finally, in Figure 4(c), we give some intuition on the type of policy our method learns using a toy example, where a user competes for attention with two other users in a follower’s feed, one with higher priority and another with lower priority. Our method learns to avoid posting whenever the user with higher priority posts.

6 Conclusions

In this paper, we approached a novel reinforcement learning problem where both actions and feedback are asynchronous stochastic events in continuous time, characterized using marked temporal point processes (MTPPs). In this problem, the policy is a conditional intensity function (and mark distribution), which is then used to sample the times (and marks) of the agent’s actions. Then, we derived a flexible policy gradient method, which does not make any assumptions on the functional form of the intensity and mark distribution of the feedback and it allows for arbitrarily complex reward functions. Experiments on two different applications in personalized teaching and viral marketing show that our method beats competing methods.

There are many interesting venues for future work. For example, we have taken a first step towards developing reinforcement learning algorithms for MTPPs, however, a natural follow up would be deriving more sophisticated reinforcement learning algorithms, *e.g.*, actor-critic algorithms, for our novel problem setting. We have evaluated in two real-world applications in personalized teaching and viral marketing, however, there are many other (high impact) applications fitting our novel problem setting, *e.g.*, quantitative trading. Finally, it would be very interesting to develop multiple agent reinforcement learning algorithms for MTPPs.

References

- [1] O. Aalen, O. Borgan, and H. Gjessing. *Survival and event history analysis: a process point of view*. Springer Science & Business Media, 2008.
- [2] M. Cha, H. Haddadi, F. Benevenuto, and P. K. Gummadi. Measuring user influence in twitter: The million follower fallacy. *ICWSM*, 10(10-17):30, 2010.
- [3] D. J. Daley and D. Vere-Jones. *An introduction to the theory of point processes: volume II: general theory and structure*. Springer Science & Business Media, 2007.
- [4] K. Doya. Reinforcement learning in continuous time and space. *Neural computation*, 12(1):219–245, 2000.
- [5] N. Du, H. Dai, R. Trivedi, U. Upadhyay, M. Gomez-Rodriguez, and L. Song. Recurrent marked temporal point processes: Embedding event history to vector. In *KDD*, 2016.
- [6] Y. Duan, X. Chen, R. Houthooft, J. Schulman, and P. Abbeel. Benchmarking deep reinforcement learning for continuous control. In *ICML*, 2016.
- [7] H. Ebbinghaus. *Memory: a contribution to experimental psychology*. Teachers College, Columbia University, 1885.
- [8] M. Farajtabar, J. Yang, X. Ye, H. Xu, R. Trivedi, E. Khalil, S. Li, L. Song, and H. Zha. Fake news mitigation via point process based intervention. In *ICML*, 2017.
- [9] N. Frémaux, H. Sprekeler, and W. Gerstner. Reinforcement learning using a continuous time actor-critic framework with spiking neurons. *PLoS computational biology*, 9(4):e1003024, 2013.
- [10] F. B. Hanson. *Applied stochastic processes and control for Jump-diffusions: modeling, analysis, and computation*, volume 13. Siam, 2007.
- [11] H. Jing and A. J. Smola. Neural survival recommender. In *WSDM*, 2017.
- [12] M. R. Karimi, E. Tavakoli, M. Farajtabar, L. Song, and M. Gomez Rodriguez. Smart broadcasting: Do you want to be seen? In *KDD*, 2016.
- [13] J. Kim, B. Tabibian, A. Oh, B. Schölkopf, and M. Gomez-Rodriguez. Leveraging the crowd to detect and reduce the spread of fake news and misinformation. In *WSDM*, 2018.
- [14] S. Leitner. So lernt man lernen: Der weg zum erfolg. *Herder*, 1972.
- [15] T. P. Lillicrap, J. J. Hunt, A. Pritzel, N. Heess, T. Erez, Y. Tassa, D. Silver, and D. Wierstra. Continuous control with deep reinforcement learning. *arXiv preprint arXiv:1509.02971*, 2015.
- [16] R. V. Lindsey, J. D. Shroyer, H. Pashler, and M. C. Mozer. Improving students’ long-term knowledge retention through personalized review. *Psychological science*, 25(3):639–647, 2014.
- [17] H. Mei and J. M. Eisner. The neural hawkes process: A neurally self-modulating multivariate point process. In *NIPS*, 2017.
- [18] E. Mettler, C. M. Massey, and P. J. Kellman. A comparison of adaptive and fixed schedules of practice. *Journal of Experimental Psychology: General*, 145(7):897, 2016.

- [19] C. Metzler-Baddeley and R. J. Baddeley. Does adaptive training work? *Applied Cognitive Psychology*, 23(2):254–266, 2009.
- [20] V. Mnih, A. P. Badia, M. Mirza, A. Graves, T. Lillicrap, T. Harley, D. Silver, and K. Kavukcuoglu. Asynchronous methods for deep reinforcement learning. In *ICML*, 2016.
- [21] H. Pashler, N. Cepeda, R. V. Lindsey, E. Vul, and M. C. Mozer. Predicting the optimal spacing of study: A multiscale context model of memory. In *NIPS*, 2009.
- [22] S. Reddy, I. Labutov, S. Banerjee, and T. Joachims. Unbounded human learning: Optimal scheduling for spaced repetition. In *KDD*, 2016.
- [23] D. E. Rumelhart, G. E. Hinton, and R. J. Williams. Learning representations by back-propagating errors. *Nature*, 323(6088):533, 1986.
- [24] B. Settles and B. Meeder. A trainable spaced repetition model for language learning. In *Proceedings of the 54th Annual Meeting of the Association for Computational Linguistics (Volume 1: Long Papers)*, volume 1, pages 1848–1858, 2016.
- [25] N. Spasojevic, Z. Li, A. Rao, and P. Bhattacharyya. When-to-post on social networks. In *KDD*, 2015.
- [26] R. S. Sutton and A. G. Barto. *Reinforcement learning: An introduction*, volume 1. MIT press Cambridge, 1998.
- [27] B. Tabibian, U. Upadhyay, A. De, A. Zarezade, B. Schoelkopf, and M. Gomez-Rodriguez. Optimizing human learning. *arXiv preprint arXiv:1712.01856*, 2017.
- [28] E. Vasilaki, N. Frémaux, R. Urbanczik, W. Senn, and W. Gerstner. Spike-based reinforcement learning in continuous state and action space: when policy gradient methods fail. *PLoS computational biology*, 5(12):e1000586, 2009.
- [29] Y. Wang, E. Theodorou, A. Verma, and L. Song. A stochastic differential equation framework for guiding online user activities in closed loop. In *AISTATS*, 2018.
- [30] Y. Wang, G. Williams, E. Theodorou, and L. Song. Variational policy for guiding point processes. In *ICML*, 2017.
- [31] D. Wierstra, A. Foerster, J. Peters, and J. Schmidhuber. Solving deep memory POMDPs with recurrent policy gradients. In *ICANN*, 2007.
- [32] R. J. Williams. Simple statistical gradient-following algorithms for connectionist reinforcement learning. *Machine learning*, 8(3-4):229–256, 1992.
- [33] A. Zarezade, A. De, U. Upadhyay, H. Rabiee, and M. Gomez-Rodriguez. Steering social activity: A stochastic optimal control point of view. *JMLR*, 2018.
- [34] A. Zarezade, U. Upadhyay, H. Rabiee, and M. Gomez-Rodriguez. Redqueen: An online algorithm for smart broadcasting in social networks. In *WSDM*, 2017.

Appendix

A Proof of Proposition 1

We first start by rewriting the expected reward function $J(\theta)$ as:

$$\begin{aligned} J(\theta) &= \mathbb{E}_{\mathcal{A}_T \sim p_{\mathcal{A};\theta}^*(\cdot), \mathcal{F}_T \sim p_{\mathcal{F};\phi}^*(\cdot)} [R^*(T)] = \mathbb{E}_{|\mathcal{A}_T|, |\mathcal{F}_T|} [\mathbb{E}_{\mathcal{A}_T, \mathcal{F}_T || \mathcal{A}_T, |\mathcal{F}_T|} [R(T) || \mathcal{A}_T, |\mathcal{F}_T|]] \\ &= \sum_{m,k} \mathbb{P}(|\mathcal{A}_T| = m) \left(\prod_{i \in \mathcal{A}_T} \int_{t_i, y_i} \lambda_\theta^*(t_i) m_\theta^*(y_i) \right) \exp \left(- \int_0^T \lambda_\theta^*(s) ds \right) \\ &\quad \times \mathbb{P}(|\mathcal{F}_T| = k) \left(\prod_{j \in \mathcal{F}_T} \int_{t_j, z_j} \lambda_\phi^*(t_j) m_\phi^*(z_j) \right) \exp \left(- \int_0^T \lambda_\phi^*(s) ds \right) R^*(T) \prod_{i \in \mathcal{A}_T} dt_i dy_i \prod_{j \in \mathcal{F}_T} dt_j dz_j, \end{aligned}$$

where we have first taken the expectation with respect to all histories conditioned on a given number of events and then taken the expectation with respect to the number of events. Then, we can compute the gradient $\nabla_\theta J(\theta)$ as follows:

$$\begin{aligned} \nabla_\theta J(\theta) &= \sum_{m,k} \nabla_\theta \left\{ \mathbb{P}(|\mathcal{A}_T| = m) \left(\prod_{i \in \mathcal{A}_T} \int_{t_i, y_i} \lambda_\theta^*(t_i) m_\theta^*(y_i) \right) \exp \left(- \int_0^T \lambda_\theta^*(s) ds \right) \right\} \\ &\quad \times \mathbb{P}(|\mathcal{F}_T| = k) \left(\prod_{j \in \mathcal{F}_T} \int_{t_j, z_j} \lambda_\phi^*(t_j) m_\phi^*(z_j) \right) \exp \left(- \int_0^T \lambda_\phi^*(s) ds \right) R^*(T) \prod_{i \in \mathcal{A}_T} dt_i dy_i \prod_{j \in \mathcal{F}_T} dt_j dz_j \\ &= \sum_{m,k} \frac{\nabla_\theta \left\{ \mathbb{P}(|\mathcal{A}_T| = m) \left(\prod_{i \in \mathcal{A}_T} \int_{t_i, y_i} \lambda_\theta^*(t_i) m_\theta^*(y_i) \right) \exp \left(- \int_0^T \lambda_\theta^*(s) ds \right) \right\}}{\mathbb{P}(|\mathcal{A}_T| = m) \left(\prod_{i \in \mathcal{A}_T} \int_{t_i, y_i} \lambda_\theta^*(t_i) m_\theta^*(y_i) \right) \exp \left(- \int_0^T \lambda_\theta^*(s) ds \right)} \\ &\quad \times \mathbb{P}(|\mathcal{A}_T| = m) \left(\prod_{i \in \mathcal{A}_T} \int_{t_i, y_i} \lambda_\theta^*(t_i) m_\theta^*(y_i) \right) \exp \left(- \int_0^T \lambda_\theta^*(s) ds \right) \\ &\quad \times \mathbb{P}(|\mathcal{F}_T| = k) \left(\prod_{j \in \mathcal{F}_T} \int_{t_j, z_j} \lambda_\phi^*(t_j) m_\phi^*(z_j) \right) \exp \left(- \int_0^T \lambda_\phi^*(s) ds \right) R^*(T) \\ &\quad \times \prod_{i \in \mathcal{A}_T} dt_i dy_i \prod_{j \in \mathcal{F}_T} dt_j dz_j \\ &= \sum_{m,k} \nabla_\theta \left\{ \log \left(\mathbb{P}(|\mathcal{A}_T| = m) \left(\prod_{i \in \mathcal{A}_T} \int_{t_i, y_i} \lambda_\theta^*(t_i) m_\theta^*(y_i) \right) \exp \left(- \int_0^T \lambda_\theta^*(s) ds \right) \right) \right\} \\ &\quad \times \mathbb{P}(|\mathcal{A}_T| = m) \left(\prod_{i \in \mathcal{A}_T} \int_{t_i, y_i} \lambda_\theta^*(t_i) m_\theta^*(y_i) \right) \exp \left(- \int_0^T \lambda_\theta^*(s) ds \right) \\ &\quad \times \mathbb{P}(|\mathcal{F}_T| = k) \left(\prod_{j \in \mathcal{F}_T} \int_{t_j, z_j} \lambda_\phi^*(t_j) m_\phi^*(z_j) \right) \exp \left(- \int_0^T \lambda_\phi^*(s) ds \right) R^*(T) \\ &\quad \times \prod_{i \in \mathcal{A}_T} dt_i dy_i \prod_{j \in \mathcal{F}_T} dt_j dz_j \\ &= \mathbb{E}_{\mathcal{A}_T \sim p_{\mathcal{A};\theta}^*(\cdot), \mathcal{F}_T \sim p_{\mathcal{F};\phi}^*(\cdot)} [R^*(T) \nabla_\theta \log \mathbb{P}_\theta(\mathcal{A}_T)] \end{aligned}$$

where we have used that $\frac{\nabla_\theta f(\theta)}{f(\theta)} = \nabla_\theta \log f(\theta)$ and

$$\log \mathbb{P}_\theta(\mathcal{A}_T) = \sum_{e_i \in \mathcal{A}_T} (\log \lambda_\theta^*(t_i) + \log m_\theta^*(z_i)) - \int_0^T \lambda_\theta^*(s) ds.$$

B Proof of Proposition 2

We first start by rewriting the penalized expected reward function $J_r(\theta)$ as:

$$\begin{aligned} J_r(\theta) &= \mathbb{E}_{\mathcal{A}_T \sim p_{\mathcal{A};\theta}^*(\cdot), \mathcal{F}_T \sim p_{\mathcal{F};\phi}^*(\cdot)} \left[R^*(T) - q_l \int_0^T g_\lambda(\lambda_\theta^*(t)) dt - q_m \int_0^T g_m(m_\theta^*(t)) dt \right] \\ &= \mathbb{E}_{\mathcal{A}_T \sim p_{\mathcal{A};\theta}^*(\cdot), \mathcal{F}_T \sim p_{\mathcal{F};\phi}^*(\cdot)} [R^*(T)] - q_l \mathbb{E}_{\mathcal{A}_T \sim p_{\mathcal{A};\theta}^*(\cdot), \mathcal{F}_T \sim p_{\mathcal{F};\phi}^*(\cdot)} \left[\int_0^T g_\lambda(\lambda_\theta^*(t)) dt \right] \\ &\quad - q_m \mathbb{E}_{\mathcal{A}_T \sim p_{\mathcal{A};\theta}^*(\cdot), \mathcal{F}_T \sim p_{\mathcal{F};\phi}^*(\cdot)} \left[\int_0^T g_m(m_\theta^*(t)) dt \right], \end{aligned}$$

where we have just used the linearity of the expectation. Then, we can use Proposition 1 and the chain rule to compute the gradient $\nabla_\theta J_r(\theta)$:

$$\begin{aligned} \nabla_\theta J_r(\theta) &= \mathbb{E}_{\mathcal{A}_T \sim p_{\mathcal{A};\theta}^*(\cdot), \mathcal{F}_T \sim p_{\mathcal{F};\phi}^*(\cdot)} [R^*(T) \nabla_\theta \log \mathbb{P}_\theta(\mathcal{A}_T)] \\ &\quad - q_l \mathbb{E}_{\mathcal{A}_T \sim p_{\mathcal{A};\theta}^*(\cdot), \mathcal{F}_T \sim p_{\mathcal{F};\phi}^*(\cdot)} \left[\int_0^T g_\lambda(\lambda_\theta^*(t)) dt \nabla_\theta \log \mathbb{P}_\theta(\mathcal{A}_T) \right] \\ &\quad - q_l \mathbb{E}_{\mathcal{A}_T \sim p_{\mathcal{A};\theta}^*(\cdot), \mathcal{F}_T \sim p_{\mathcal{F};\phi}^*(\cdot)} \left[\int_0^T g'_\lambda(\lambda_\theta^*(t)) \nabla_\theta \lambda_\theta^*(t) dt \right] \\ &\quad - q_m \mathbb{E}_{\mathcal{A}_T \sim p_{\mathcal{A};\theta}^*(\cdot), \mathcal{F}_T \sim p_{\mathcal{F};\phi}^*(\cdot)} \left[\int_0^T g_m(m_\theta^*(t)) dt \nabla_\theta \log \mathbb{P}_\theta(\mathcal{A}_T) \right] \\ &\quad - q_m \mathbb{E}_{\mathcal{A}_T \sim p_{\mathcal{A};\theta}^*(\cdot), \mathcal{F}_T \sim p_{\mathcal{F};\phi}^*(\cdot)} \left[\int_0^T g'_m(m_\theta^*(t)) \nabla_\theta m_\theta^*(t) dt \right] \\ &= \mathbb{E}_{\mathcal{A}_T \sim p_{\mathcal{A};\theta}^*(\cdot), \mathcal{F}_T \sim p_{\mathcal{F};\phi}^*(\cdot)} \left[\begin{aligned} &\left(R^*(T) - q_l \int_0^T g_\lambda(\lambda_\theta^*(t)) dt - q_m \int_0^T g_m(m_\theta^*(t)) dt \right) \nabla_\theta \log \mathbb{P}_\theta(\mathcal{A}_T) \\ &- \left(q_l \int_0^T g'_\lambda(\lambda_\theta^*(t)) \nabla_\theta \lambda_\theta^*(t) dt + q_m \int_0^T g'_m(m_\theta^*(t)) \nabla_\theta m_\theta^*(t) dt \right) \end{aligned} \right] \end{aligned}$$

where $g'_\lambda(\lambda_\theta^*(t)) = \frac{d g_\lambda(\lambda_\theta^*(t))}{d \lambda_\theta^*(t)}$ and $g'_m(m_\theta^*(t)) = \frac{d g_m(m_\theta^*(t))}{d m_\theta^*(t)}$.

C Sampling event times from the intensity $\lambda_\theta^*(t)$

Immediately after taking an action at time t_i , the agent has to determine the time of the next action t_{i+1} by sampling from the intensity function $\lambda_\theta^*(t)$ given by Eq. 5. However, if a feedback event arrives at time $s < t_{i+1}$, *i.e.*, the feedback event arrives *before* the agent has performed her next action, then the intensity function $\lambda_\theta^*(t)$ will need to be updated and the time t_{i+1} will not be a valid sample from the updated intensity. To overcome this difficulty, we design the following procedure, which to the best of our knowledge, is novel in the context of temporal point processes. Recall that the intensity function of the action events was

$$\lambda_\theta^*(t) = \exp(b_\lambda + \mathbf{V}_h \mathbf{h}_i) \exp(\omega_t(t - t_i)) \tag{11}$$

In other words, we write $\lambda_\theta^*(t) = c \cdot e^{\omega t(t-t_i)}$ and c changes due to an arrival of an event. So, we can state our problem as the following more general problem of sampling from a partially known intensity function:

$$\lambda(t) = \begin{cases} c_1 e^{-\omega(t-t_i)} & \text{if } t < s \\ c_2 e^{-\omega(t-t_i)} & \text{otherwise,} \end{cases} \quad (12)$$

where the parameters c_1 is known to us at time t_i but s, c_2 are revealed to us only at time s , *i.e.*, if our sampled time is greater than s . Due to this, we cannot sample from the above intensity using simple rejection sampling or the superposition property of poisson processes, as previous work [27, 34]. Instead, at a high level, we solve the problem by first sampling a uniform random variable $u \sim U[0, 1]$ and then using it to calculate $t_{i+1} = CDF_1^{-1}(u | c_1, t_i)$, where $CDF_1(t | c_1, t_i)$ denotes the cumulative distribution function of the next event time. Here, we are using inverse transform sampling under the assumption that the intensity function is defined completely using c_1 only. Then, we wait until the earlier of either t_{i+1} , when we *accept* the sample, or s , in which case the parameters c_2 are revealed to us. With the full knowledge of the intensity function, we can now *refine* our sample $t_{i+1} \leftarrow CDF_2^{-1}(t | c_1, t_i, c_2, s)$ re-using the same u that we had originally sampled.

To be able to perform the above procedure in an efficient manner, we should be able to express $CDF_1^{-1}(t | c_1, t_i)$ and $CDF_2^{-1}(t | c_1, t_i, c_2, s)$ analytically. Perhaps surprisingly, we can indeed express both functions analytically for our parametrized intensity function, given by Eq. 12, *i.e.*,

$$CDF_1(t | c_1, t_i) = \Pr[\text{An event happens before } t] = 1 - \Pr[\text{No event in } (t_i, t)]$$

$$= 1 - \exp\left(-\int_{t_i}^t \lambda(\tau) d\tau\right)$$

$$= 1 - \exp\left(-\int_{t_i}^t c_1 e^{-\omega(\tau-t_i)} d\tau\right)$$

$$= 1 - \exp\left(\frac{c_1}{\omega}(e^{-\omega(t-t_i)} - 1)\right)$$

$$\implies CDF_1^{-1}(u | c_1, t_i) = t_i - \frac{1}{\omega} \log\left(1 + \frac{\omega}{c_1} \log(1-u)\right) \quad (13)$$

$$\text{Similarly, } CDF_2^{-1}(u | c_1, t_i, c_2, s) = s - \frac{1}{\omega} \log\left(1 + \frac{\omega}{c_2} \log\left(\frac{1-u}{Q}\right)\right) \quad (14)$$

$$\text{where } Q = \exp\left(-\frac{c_1}{\omega}(1 - \exp(-\omega(s-t_i)))\right).$$

Notice that Eq. 14 is the same as Eq. 13, if our uniform sample had been $u' = 1 - \frac{1-u}{Q}$, and we had started the sampling process at time s instead of time t_i with parameters c_2, ω . Using this insight, we can easily generalize this sampling mechanism to account for an arbitrary number of feedback events occurring between two actions of the agent. Algorithm 2 summarizes our sampling algorithm, where COMPUTEC1 and COMPUTEC2 compute the current values of c_1 and c_2 , respectively, WAITUNTILNEXTFEEDBACK(t) sets a flag e to True if a feedback event (s, z) happens before time t . Remarkably, given a cut-off time T , the algorithm only needs to sample $|\mathcal{A}_T|$ times from a uniform distribution and perform $O(|\mathcal{H}_T|)$ computations.

Finally, note that, in the above procedure, there is a possibility that the inverse CDF functions may not be completely defined on the domain $[0, 1]$. This would mean that the agent's MTPP may go *extinct*, *i.e.*, there may be a finite probability of the agent not taking an action after time t_i at all. In such cases, we assume that the next action time is beyond our episode horizon T ,

Algorithm 2: It returns the next action time

```

1: Input: Time of previous action  $t'$ , history  $\mathcal{H}_{t'}$  up to  $t'$ , cut-off time  $T$ 
2: Output: Next action time  $t$ 
3:  $c_1 \leftarrow \text{COMPUTEC1}(\mathcal{H}_{t'})$ 
4:  $t \leftarrow CDF_1^{-1}(u | c_1, t')$ 
5: while  $t < T$  do
6:    $(e, s, z) \leftarrow \text{WAITUNTILNEXTFEEDBACK}(t)$ 
7:   if  $e == \text{True}$  then
8:      $\mathcal{H}_{t'} \leftarrow \mathcal{H}_{t'} \cup \{(s, z)\}$ 
9:      $c_1 \leftarrow \text{COMPUTEC1}(\mathcal{H}_{t'}), c_2 \leftarrow \text{COMPUTEC2}(\mathcal{H}_{t'})$ 
10:     $t \leftarrow CDF_2^{-1}(u | c_1, t', c_2, s)$ 
11:   else
12:     return  $t$ 
13:     break
14:   end if
15: end while
16: return  $t$ 

```

Application	N_b	N_e	T	l_r	D_i	D_h	q_l	q_m
Spaced repetition	5000	32	14 days	$\frac{0.02}{1+2i \cdot 10^{-3}}$	8	8	10^{-2}	$5 \cdot 10^{-3}$
Smart broadcasting	1000	16	It varies across users	$\frac{10^{-2}}{1+i \cdot 10^{-4}}$	8	8	0.33 (100)	–

Table 1: Hyperparameter values used in the implementation of our method for smart broadcasting and spaced repetition. In smart broadcasting, $q_l = 0.33$ for top-1 inverse chronological ordering and $q_l = 100$ for average rank inverse chronological ordering.

but we will save the original u and will keep calculating the inverse CDF using it as, due to the non-linear dependence of the parameters on the history, the samples may become finite again.

D Experimental details

We carried out all our experiments using TensorFlow 1.8.1 and we implemented stochastic gradient descent (SGD) using the Adam optimizer, which achieved good performance in practice, as shown in Figure 5. Therein, we had to specify eight hyperparameters: (i) N_b – the number of batches, (ii) N_e – the number of episodes in each batch, (iii) T – the time length of each episode, (iv) l_r – the learning rate, (v) D_i – the dimension of vectors $\mathbf{W}_\bullet, \mathbf{b}_\bullet$'s in the input layer, (vi) D_h – the dimension of the hidden state \mathbf{h}_i , (vii) q_l – the value of the regularizer coefficient for intensity function, (viii) q_m – the value of the regularizer coefficient for mark distribution. Note that, the dimensions of the other trainable parameters $\mathbf{W}_h, \mathbf{W}_1, \dots, \mathbf{W}_4$ and \mathbf{b}_h in the hidden layer depend on D_i and \mathbf{V}_λ and \mathbf{V}_c^y in the output layer depend on D_h , which we selected using cross validation. The values for both applications—spaced repetition and smart broadcasting—are given in Table 1.

We run the spaced repetition experiments using a Tesla K80 GPU on a machine with 32 cores and 500GB RAM. With this configuration, for episodes with up to ~ 2000 events, the training process takes ~ 5 seconds in average to run one iteration of SGD with batch size $N_e = 32$. We run the smart broadcasting experiments on 2 CPU cores of an Intel(R) Xeon(R) CPU E5-2680 v2 @ 2.80GHz and 20GB RAM. With this configuration, for feeds sorted algorithmically and episodes with up to ~ 250 events, the training process takes ~ 30 seconds to run one iteration of SGD with batch size $N_e = 16$.

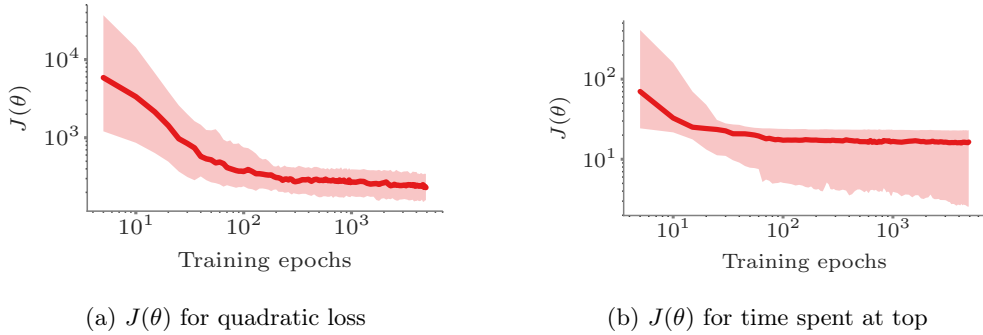


Figure 5: The cost-to-go $J(\theta)$ calculated on the held-out test-set for different loss functions during training falls quickly with the number of epochs.

E Student model

We use the student model proposed by Tabibian *et al.* [27], which is an improved version of the student model proposed by Settles *et al.* [24]. To accurately predict the student’s ability to recall an item, the model accounts for the item difficulty, the history of reviews (and recalls) by the student, and the time since the last review.

More formally, the probability $m_i(t)$ that an item i , which was last reviewed at time η , will be successfully recalled at time t is given by:

$$m_i(t) = e^{-n_i(t) \times (t-\eta)} \quad (15)$$

where $n_i(t)$ denotes the forgetting rate for the item i . The rate of forgetting an item depends on the inherent difficulty of the item, denoted by $n_i(0)$, but also on whether the user was able to recall the item successfully in the past or not. More specifically, the model has two additional parameters α and β , which determine by how much the forgetting rate ought to change if the student recall, or fails to recall, the item on a review at time t , *i.e.*,

$$n_i(t) = \begin{cases} (1 - \alpha) \times n_i(t^-) & \text{if recalled} \\ (1 + \beta) \times n_i(t^-) & \text{if forgotten} \end{cases} \quad (16)$$

In our work, the parameters α and β , as well as the initial item difficulty $n_i(0)$, are learned using historical learning data from Duolingo as in Tabibian *et al.* [27].

Note that we have picked this student model for its simplicity but relatively good predictive power, as shown by previous work. Several other student models have also been proposed in literature, ranging from exponential [7] to more recent multi-scale context models (MCM) [21], which are biologically inspired and can explain a wider variety of learning phenomenon. Since our methodology is agnostic to the choice of student model, it would be very interesting to experiment with other student models.

F Feed sorting algorithm

We use a feed sorting algorithm inspired by the *in-case-you-missed-it* feature, which is now prevalent in a variety of social media sites, notably Twitter at the time of writing. Our sorting algorithm divides each user’s feed in two sections: (i) a prioritized section at the top of the user’s feed, where messages are sorted according to the *priority* of the user who posted the message, and (ii) a bulk section, where messages are sorted in reverse chronological order. In the above,

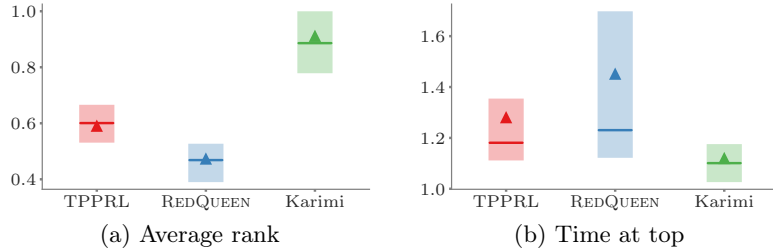


Figure 6: Performance of our policy gradient method against REDQUEEN [34] and Karimi’s method [12] on feeds sorted in reverse chronological order. Panels (a) and (b) show the average rank and time at the top, where the solid horizontal line shows the median value across users, normalized with respect to the value achieved by a user who follows a uniform Poisson intensity, and the box limits correspond to the 25%-75% percentiles. For the average rank, lower is better and, for time at the top, higher is better. In both cases, the number of messages posted by each method is the same.

each post stays for a fixed time τ in the prioritized section and then it moves to the inverse chronological section. Moreover, note that if the prioritized section contains several messages from the same user, they are sorted chronologically.

In our experiments, for each user’s feed, we set the priority of the users she follows inversely proportional to her level of activity, as more active users will naturally appear on the feed while users with sporadic posting activity may need more promotion, we set the priority of the user under our control to be at the median priority among all users posting in the feed, and set τ to be approximately 10% of the prioritized lifetime of posts $\tau = 0.1T$, where T is the time length of each sequence.

G Experiments on feeds sorted in reverse chronological order

We follow the same experimental setup as in Section 5, however, feeds are sorted in reverse chronological order. Figure 6 summarizes the results, where the number of messages posted by each method is the same and all rewards are normalized by the reward achieved by a baseline user who follows a uniform Poisson intensity. The results show that our method is able to achieve competitive results in comparison with REDQUEEN, which is an online algorithm specially designed to minimize the average rank in feeds sorted in reverse chronological order, and it outperforms Karimi’s method, which is an offline algorithm specially designed to maximize the time at the top in feeds sorted in reverse chronological order.

H Baseline with $w_t = 0$

We also explored how our algorithm performs when we force the w_t parameter to be zero, *i.e.*, we force the policy to be piece-wise constant between feedback and action events. To this end, we retrained the neural networks by doing a parameter sweep over q_l (and q_m for the spaced repetition experiments) and picked those values which arrived to roughly the same number of events as produced by the policy learned by the network where we do not constraint $w_t = 0$.

The resulting baseline is shown in Figure 7 for both the smart broadcasting (Figures 7a and 7b) and spaced repetition experiments (Figures 7c and 7d). We see that forcing the policy to be piecewise constant degrades performance and increases the variance in both settings, as expected. In the smart broadcasting experiments, the mean (median) relative decrease in average rank is

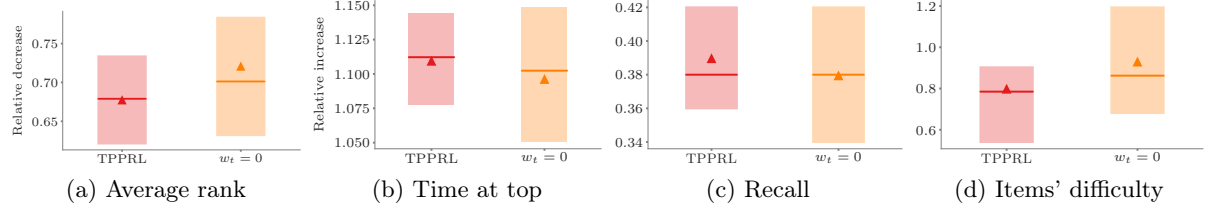


Figure 7: Comparing against piece-wise constant ($w_t = 0$) baseline. In all figures, the solid horizontal line shows the median value across users and the box limits correspond to the 25%-75% percentiles. Panels (a) and (b) show the average rank and time at the top for the smart broadcasting experiments, respectively. The values are normalized with respect to the value achieved by a user who follows a uniform Poisson intensity. For the average rank, lower is better and, for time at the top, higher is better. In both cases, the number of messages posted by each method is the same within a 10% tolerance. Panel (c) shows the empirical recall probability at test time and Panel (d) shows the distribution of the difficulty of items chosen by our method and the baseline version for the space repetition experiments. The total number of learning events (across all items) are within 5% of each other in the two settings.

33% (33%) for our method TPPRL, while it is 28% (30%) for the $w_t = 0$ baseline. Similarly, the increase in mean time spent at the top is about 11% for our method (TPPRL), while it is 9% for the $w_t = 0$ baseline. In the spaced repetition experiment, we see that the mean recall falls from 38.9% to 37.9%. The difference in policy learned is especially notable in Figure 7d where we see that the agent, when constrained to $w_t = 0$, learns to spread its attempts over a wider set of items, which have higher difficulty than the items selected by the unconstrained policy.